Volume 1 | Number 1 | Jan 2013 | Pages 1–100

Nanoscale

www.rsc.org/nanoscale

ROYAL SOCIETY OF CHEMISTRY

ROYAL SOCIETY OF CHEMISTRY

www.rsc.org/nanoscale

Journal Name

ARTICLE

Intelligent Janus Nanoparticle for Intracellular Real-time Monitoring Dual Drug Release

Han Cao,[a] Yuhong Yang,*[b] Xin Chen,[a] Zhengzhong Shao*[a]

Stimuli-responsive nanomaterials have been receiving much attention as drug delivery carriers, however, understanding of multi-drugs releasing from the carriers for efficient therapeutics is highly challenging. Here, we report a novel nanosystem, Janus particle Dox-CMR-MS/Au-6MP (Dox: doxorubicin, CMR: 7-hydroxycoumarin-3-carboxylate, MS: mesoporous silica, Au: gold, 6MP: 6-mercaptopurine) with opposing MS and Au faces, which can monitor intracellular dual-drug (Dox and 6MP) controlled release in real time based on fluorescence resonance energy transfer (FRET) and surface-enhanced Raman scattering (SERS). FRET acceptor Dox is attached to CMR (as FRET donor) conjugated MS by a pH-responsive linker hydrazone, and 6MP is conjugated to the Au surface through gold-thiol interaction. As the Janus nanoparticle enters into tumor cells, the breakage of hydrazone bond in acidic environment and the substitution of glutathione (GSH) overexpressed in cancer cells give rise to the release of Dox and 6MP, respectively. Thus, the changes of CMR fluorescence signal and the SERS decrease of 6MP can be used to monitor the dual-drug release within living cells in real time. In addition, the work demonstrates the enhanced anticancer effect of the designed dual-drug loaded nanosystem. Therefore, the current study may open up new perspectives to real-time study of intelligent multi-drug delivery and release, as well as the cellular responses to drug treatment.

Introduction

Utilizing multifunctional drug delivery system (MDDS) is emerging as a promising approach to improve the efficacy of chemotherapy.[1] The therapeutic efficacy of drugs transported by nanocarriers not only depends on their accumulation at the focus, but is also strongly affected by their release property. Therefore, besides tracing drug delivery, it is important to develop protocols to get details of drug release within cells.[2] This is a rather challenging task as it requires to the design of ingenious and smart nanomaterials which can generate contrast changes in response to the release of the drug from the carrier.[3] Optical imaging strategy is an appropriate tool to elucidate key details of the drug release process being highly sensitive to the microenvironment.[4] Several drug delivery systems (DDS) have already been developed for monitoring drug release based on fluorescence resonance energy transfer (or Förster resonance energy transfer, FRET)[5,6] or surface-enhanced Raman scattering (SERS).[7, 8] FRET is a well-established energy transfer process between two fluorophores, which is very sensitive to monitor the changes in the donor-to-acceptor separation distance at the nanoscale

(generally less than 10 nm).[9] SERS can enhance the Raman signals of molecules adsorbed on Au or Ag metallic nanostructures by 6-14 orders of magnitude.[10,11] Some non-optical techniques, such as magnetic resonance imaging (MRI), have also been employed to trace drug delivery.[12] It is well known that most conventional anticancer drugs show a narrow therapeutic window because of the cytotoxicity arise from the nonspecific biodistribution and multi-drug resistance. Current treatment options in clinic and research to chemotherapy are exploiting combined therapy with dual or even multiple anticancer agents to improve therapeutic efficacy.[13-16] However, to the best of our knowledge, most of previous studies focused on the real-time monitoring the release of a single drug in cells.[17-19] While real-time monitoring the release of multi-drugs intracellularly is more challenging because the generated signals of multiple drugs releasing from the carrier should never affect each other. Besides, controlling the release of each drug independently is also a great challenge for combined therapy.[20] Therefore, it is of considerable importance to develop a new smart nanoplatform that is able to realize the specific targetability and traceable multiple drug delivery and controlled release intracellularly. As both FRET and SERS are based on distances between two molecules or substances, they are potentially ideal for the determination of delicate interactions between nanocarries and external/internal stimuli.

Janus nanoparticle (Janus NP) possesses multiple surface structures that can be anisotropic in shape, composition, surface chemistry, etc.[21] Therefore, it is able to provide drastically different chemical or physical property and directionality easily within a single particle.[22] Compared with

[a] State Key Laboratory of Molecular Engineering of Polymers, Department of Macromolecular Science and Laboratory of Advanced Materials and [b] Research Center for Analysis and Measurement, Fudan University, Shanghai, 200433, P. R. China

Nanoscale Accepted Manuscript

other nanosystems with uniform surface structure, Janus NP is more convenient to assemble multiple components in a single delivery system to realize multimodal imaging and combined therapy of two or more drugs.[23] As a proof-of-concept, we developed a multifunctional nanosystem, Janus Dox-CMR-MS/Au-6MP (Dox: doxorubicin, CMR: 7-hydroxycoumarin-3-carboxylate, MS: mesoporous silica, Au: gold, 6MP: 6-mercaptopurine) nanoparticle (shortened as Janus Dox/6MP NP throughout the text) with opposing MS and Au faces, for real-time monitoring the responsive release of dual drugs (Dox and 6MP) intracellularly based on FRET and SERS. Dox (as FRET acceptor) is attached to nanochannel walls of CMR (as FRET donor) functionalized MS by a pH-responsive linker hydrazone. In the meantime, 6MP is conjugated to the Au surface through a gold-thiol interaction. When Janus Dox/6MP NPs enter the tumor cells, the breakage of hydrazone bond in acidic environment and the substitution of glutathione (GSH) overexpressed in most cancer cells give rise to the release of Dox and 6MP, respectively (Figure 1). Consequently, confocal microscopy and Raman spectrometer with dark-field microscopy (DFM) are used to detect the fluorescence recovery of CMR and the SERS decrease of 6MP, respectively, to monitor dual drugs release within living cells in real time. In addition, the designed dual-drug loaded NP demonstrates remarkably enhanced anticancer efficiency compared with single drug loaded NPs. Therefore, we believe the present study opens up a new perspective to real-time study of intelligent multi-drug delivery and release, as well as the cellular responses to drug treatment.
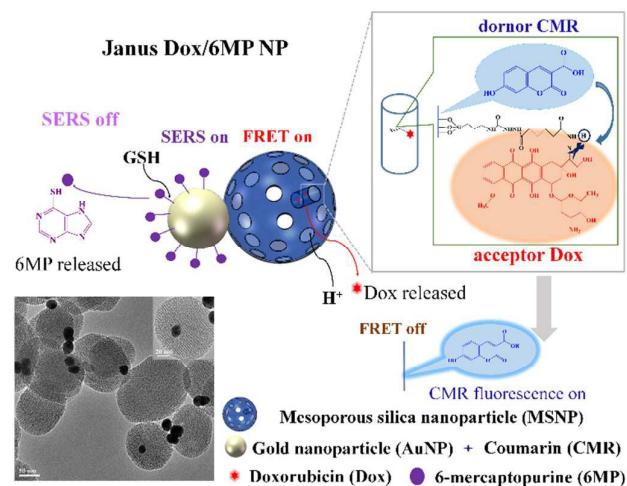
Figure 1. Schematic representation of Janus Dox/6MP NP and the mechanism of real-time monitoring dual drugs with pH/redox dual responsive release in living cells. The framework of MS is functionalized with CMR and the nanochannel walls are modified with Dox by pH-responsive linkers hydrazone. The Au surface is conjugated with 6MP by gold-thiol bond. After entering tumor cells, the breakage of hydrazone bond at acidic environment and the overexpressed GSH trigger the release of Dox and 6MP, separately. The FRET and SERS on/off

process can be used to monitor the dual-drug release within living cells in real time.

Results and discussion

### Preparation and Characterization of Janus Dox/6MP NP.

The Janus Dox/6MP NPs were prepared by Pickering emulsion template method[24] with some modifications. Firstly, CMR incorporated MS (CMR-MS) was synthesized through sol-gel co-condensation of tetraethoxysilane (TEOS) and CMR-conjugated 3-aminopropyltrimethoxysilane (APTS) in the presence of cetyltrimethylammonium bromide (CTAB) and NaOH. Afterwards, CTAB was removed by extraction in methanol/HCl solution. CMR-MS nanoparticles were then partially confined at the interface of a Pickering emulsion using paraffin as the oil phase. The exposed nanoparticle surface was further modified with (3-mercaptopropyl) trimethoxysilane, and then attached on 6MP coated Au nanoparticles (Au-6MP). A stable anisotropic CMR-MS/Au-6MP colloid nanoparticle (shortened as Janus 6MP NP throughout the text) was formed by dissolving paraffin in diethyl ether. To conjugate Dox onto MS nanochannel walls of Janus 6MP NP, a silanehydrazide crosslinker was firstly synthesized by reacting APTS with adipic acid dihydrazide, thus Dox was able to covalently attached via the formation of hydrazone bond that was cleavable at endosomal/lysosomal pHs.[25] TEM image (Figure 1) clearly indicates the formation of anisotropic nanostructure of Janus Dox/6MP NP with diameter around 130 nm (also can be confirmed by dynamic light scattering, Figure S1).

Fourier transform infrared (FTIR) spectroscopy was employed to characterize the chemical bonds and surface groups formed on these Janus NPs (Figure S2). The FTIR spectra of the CMR-MS and Janus Bare NP (i.e. bare Janus nanoparticle without loading drugs) were similar to those reported for MS nanoparticles,[25] indicating only the surface silanol groups and low-frequency silica vibrations. The hydrazone bond from the conjugation of Dox in Janus NP only loaded Dox (Janus Dox NP) is confirmed by the overlapping absorption peaks of imine (C=N) and the amide I band at 1657 cm^{-1} as well as the amide II band at about 1553 cm^{-1}.[25] The surface area and pore size of the Janus NPs were determined by Brunauer–Emmett–Teller (BET) and Barrett–Joyner–Halenda (BJH) analysis. The results show that BET pore volume and BJH pore diameter decrease due to the functionalization process (Table S1 and Figure S3). The drug loading percentage of Dox and 6MP by weight in the Janus Dox/6MP NP was 1.96% and 1.18% respectively by detecting the unloaded drug in the supernatant.

Fluorescence/Raman and Responses of Janus Dox/6MP NP.

The hydrazone bond is stable in normal physiological conditions (even in blood), but can be rapidly broken in endo/lysosomes of cancer cells where pH value is around 5-6. As Dox is a fluorescent quencher for coumarin derivatives,[26]

ARTICLE

we assume that the efficient FRET between CMR and Dox takes place before drug release, thus enabling us to monitor the release of Dox in real-time by the fluorescence recovery of CMR. To verify this, the fluorescence emission spectrum of CMR and the UV-Vis absorption spectrum of Dox were obtained. It shows that when CMR is excited at 405 nm, it generates an emission in the range of 420-550 nm. Therefore, CMR upon excitation at 405 nm was able to act as a photon donor for Dox which absorbs maximally at 480 nm (Figure S4). Figure 2A is the emission spectra (λ_{em} = 450 nm) of CMR from the Janus Dox/6MP NPs in PBS buffer (pH = 5). The spectra show that the intensity is weak at the beginning, and then increases significantly with time, while the intensity of Dox in the emission spectra (λ_{em} = 595 nm) decreases with time. To further confirm that acidic pH values only triggers the release of Dox whereas CMR is still stabilized within Janus Dox/6MP NPs against the leaching by endosome pHs, we investigated CMR fluorescence in the sample without Dox (i.e. Janus 6MP NP) on excitation at 405 nm. The intensity of CMR within Janus 6MP NPs in PBS solution (pH = 5) changes little during the incubation (Figure 2B), indicating that CMR can hardly release from the Janus NP. Therefore, the fluorescence increase of CMR in Janus Dox/6MP NP is entirely due to the release of Dox and the decreasing of FRET efficacy.
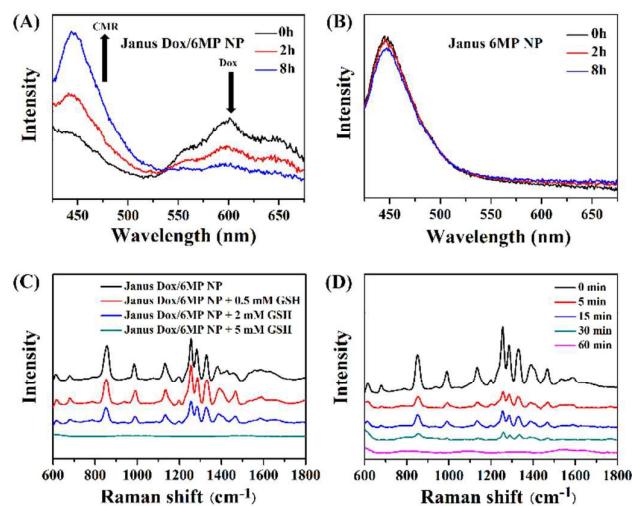

Figure 2. Fluorescence spectra of (A) Janus Dox/6MP NPs and (B) Janus 6MP NPs, incubated with PBS (pH = 5). The two arrows mean that CMR fluorescence increased with time while Dox fluorescence decreased with time. SERS spectra of Janus Dox/6MP NPs incubated with (C) PBS or different concentrations of GSH after 1 h, (D) 5 mM GSH for different times.

On the other hand, 6MP was reacted on the gold side of Janus Dox/6MP NP via gold-thiol reaction. Figure 2C shows the SERS spectra of 6MP on Janus Dox/6MP NPs in solution with different amounts of GSH. As it is well-known that GSH overexpresses in most cancer cells, it is often used as an endogenous trigger to release drug molecules.[27] As the pristine 6MP, GSH and Janus Dox NP do not exhibit obvious Raman responses (Figure S5), the Raman peaks shown in Figure 2C should come from 6MP that is enhanced by gold contained Janus NPs. It clearly demonstrates that the SERS intensity of 6MP in Janus Dox/6MP NP declines rapidly with the increase in GSH concentration (the nanoparticles were treated with GSH for 1 h). SERS spectra of Janus Dox/6MP NPs didn't change with time when incubated with PBS (pH = 5.0) (Figure S6A), demonstrating that the released Dox had no effect on monitoring 6MP through SERS spectra. On the other hand, Figure 2D shows that SERS intensity of 6MP gradually decreases with the incubation time in 5 mM of GSH. While Raman spectra of Janus Dox NPs had no change when incubated with 5 mM of GSH (Figure S6B), illustrating that decrease of SERS intensity of Janus Dox/6MP NPs incubated with 5 mM of GSH only resulted from the release of 6MP. The intensity of 6MP in SERS spectra changes from strong to almost negligible in the presence of 5 mM GSH from the beginning to 1 h, indicating that our Janus Dox/6MP NP has the ability to monitor the release of 6MP.

pH/redox Responsive Drug Release.

From the results discussed above, there are two kinds of responsive release mechanism (pH and redox) involved in our system, both of which are commonly used to trigger the drug release in constructing DDS for cancer treatment.[28, 29] Therefore, it is necessary to evaluate the characteristics of pH/redox responsive drug release from the Janus Dox/6MP NP before the establishment of drug release monitoring method. Firstly, the release profiles of Dox at different pH values are presented in Figure 3A, showing that the release rate and the amount of Dox from the Janus Dox/6MP NP increase rapidly with the acidity. For example, 5% of Dox was released at pH 7.4, 15% at pH 6.5, and 60% at pH 5.0 within 24 h. The minimal release of Dox under normal physiological conditions (pH 7.4) implies few unwanted drug is released during blood circulation because of the stability of the hydrazone bond linker at pH 7.4, which can reduce the side effects of Dox significantly.
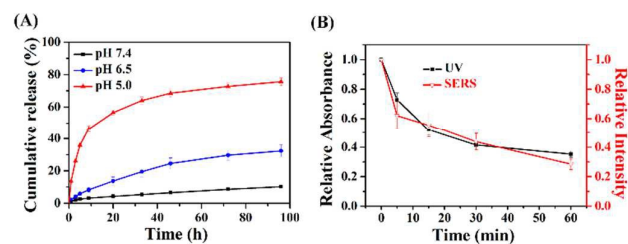

Figure 3. In vitro (A) Dox release at different pH values by quantifying fluorescence of Dox supernatant and (B) 6MP release after treated with 5 mM of GSH by evaluating decrease of SERS intensity and UV-Vis absorption.

In the meantime, the release of 6MP from the Janus Dox/6MP NP can be monitored by the change of Raman intensity at 1258 cm^{-1} (i.e., the characteristic C−N stretching vibration of the purine ring in 6MP) in SERS. UV-Vis absorption spectroscopy can be also used to verify the SERS results. Figure 3B shows the decrease of SERS intensity at 1258 cm^{-1} fits well with the decrease of UV-Vis absorbance of 6MP at 323 nm (where no obvious Dox absorbance was observed, Figure S7) after normalization, confirming the possibility for the intracellular SERS monitoring drug release.

### Intracellular Monitoring/imaging Drug Release.

Confocal microscopy was used to investigate the real-time monitoring of our Janus Dox/6MP NPs in living cells by determining the fluorescence change of the nanoparticles incubated with HeLa cells. Figure 4 shows that the blue fluorescence (CMR) increases with time from 0 to 8 h due to the Dox release from NPs by cleavage of hydrazone bond in endo/lysosome pH (pH 5-6), weakening the quenching effect of the donor CMR. In addition, as the lysosomes of the cells were stained with green fluorescent lysotracker, the co-localization (merged images) of blue (CMR), green (lysosome) and red fluorescence (Dox) demonstrates that nanoparticles are internalized and cleaved in lysosomes. These results agree with the fluorescence recovery experiment in PBS solutions shown in Figure 2A.
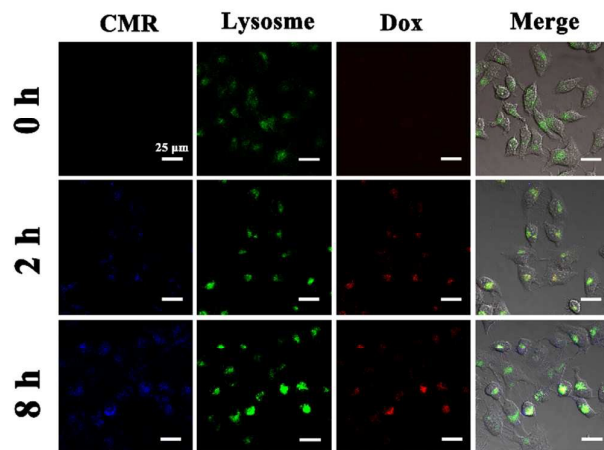
Figure 4. Real-time monitor Dox release by confocal microscopy. HeLa cells were treated with 100 µg/mL of Janus Dox/6MP NPs. Scale bar, 25 µm.

In the meantime, Raman spectrometer equipped with DFM was applied to monitor 6MP release triggered by GSH from Janus Dox/6MP NPs in HeLa cells in real-time, by detecting the changes of SERS intensity. As shown in Figure 5, the DFM images and corresponding SERS spectra at a certain local point inside a single HeLa cell after the uptake of the Janus Dox/6MP

NPs confirm the internalization of NPs convincingly. As an addition proof, the SERS intensity of 6MP on Janus Dox/6MP NPs decreased with the time when 5 mM of glutathione monoester (GSH-OEt) was infused,[27] which confirms the GSH-mediated 6MP release in the cells (Figure 5, Figure S8). Therefore, by using confocal microscopy and DFM combined Raman spectroscopy, we are able to monitor the stimulated release of dual drugs in living cells in real time through our new-developed Janus Dox/6MP NP.
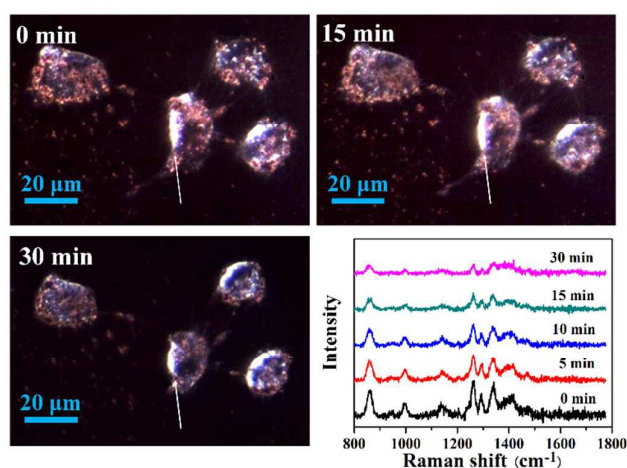
Figure 5. Real-time DFM images and SERS spectra monitoring 6MP release from Janus Dox/6MP NP in HeLa cells incubated with 5 mM of GSH-OEt. The arrows indicate the position where the SERS spectra were obtained.

In vitro Cell Viability with Combined Efficacy.

The cytotoxicity of our Janus NPs was assessed in HeLa cells by using a colorimetric cell viability assay. The viability of HeLa cells after exposure to the Janus Bare NPs maintains at more than 90% even when the nanoparticle concentration reaches 500 µg/mL (Figure 6A), indicating the excellent biocompatibility of such Janus NP. As expected, the Janus NPs loading drugs exhibits remarkable cytotoxicity. Moreover, the Janus Dox/6MP NP, which conjugated both Dox and 6MP, displayed remarkably enhanced efficiency in killing cancer cells compared with single drug loaded nanoparticles (Janus Dox NP and Janus 6MP NP) as shown in Figure 6B.
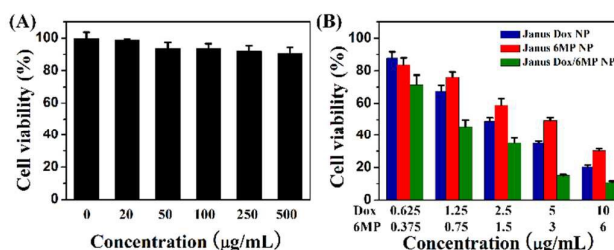
Figure 6. In vitro cytotoxicity of (A) Janus Bare NPs and (B) Janus Dox NPs, Janus 6MP NPs and Janus Dox/6MP NPs incubated with HeLa cells for 48 h at different concentrations.

Compared with free drugs, drug loaded Janus NP exhibited lower IC$_{50}$ (concentration of drug required to kill 50% of cells) values (Table S2 and S3) for Hela cells. But there was an exception, i.e. IC$_{50}$ of 6MP in Janus Dox/6MP NP was a little higher than in the mixture of free Dox and 6MP, which may attribute to the different release rate of dual drugs from Janus NPs. The cytotoxicity of the drug loaded Janus NPs in another cancer cell line MDA-MB-231 were also tested (Figure S9), and the results are similar to those in HeLa cells, declaring the versatility of our multifunctional Janus Dox/6MP NP.

Conclusions

In summary, a multifunctional Janus Dox/6MP NP has been successfully developed for real-time monitoring intracellular dual-drug stimuli-responsive release based on FRET and SERS. The asymmetric Janus NP is composed of opposed mesoporous silica and gold, which are separately functionalized with FRET pair CMR/Dox and 6MP either by pH or redox responsive bond. Fluorescence and Raman results confirm that Dox and 6MP were able to release from Janus Dox/6MP NPs in solutions with addition of acid and GSH respectively. More importantly, the cell experiments successfully demonstrate that Dox and 6MP dual-drug responsive release is able to be real-time monitored within living cells by detecting the changes of FRET signals of CMR/Dox with confocal microscopy and the decrease of SERS intensity of 6MP in Raman combined DFM spectroscopy. Moreover, the enhanced anticancer effect of the dual drug loaded Janus NP is accomplished compared with single drug loaded Janus NPs. The Janus Dox/6MP NP for real-time monitoring the controlled release of dual drugs in living cells may lead to further development of a new concept for intelligent nano-drug carriers, allowing more opportunities in cancer theranostics.

Experimental Section

Materials

Hexadecyltrimethylammonium bromide (CTAB, 99%), tetraethoxysilane (TEOS), aminopropyltrimethoxysilane (APTS), Pluronic F127 and glutathione ethyl ester (GSH-OEt) were purchased from Sigma-Aldrich. N-Succinimidyl 7-Hydroxycoumarin-3-carboxylate (CMR) was purchased from J&K Chemical Co., Ltd. Chloroauric acid tetrahydrate was purchased from Sinopharm Chemical Reagent Co., Ltd. (Shanghai, China). Sodium hydroxide, trisodium citrate, (3-mercaptopropyl)trimethoxysilane, 3-(triethoxysilyl)propyl isocyanat, adipic acid dihydrazide, paraffin, trifluoroacetic acid, 6-mercaptopurine were purchased from Aladdin Industrial Inc. Doxorubicin hydrochloride was purchased from Dalian Meilun

Biology Technology Co., LTD. (Dalian, China). CCK-8 was purchased from Dojindo Laboratorise, Japan. Gibco® fetal bovine serum (FBS), Gibco® DMEM and LysoTracker® Probes labeling kit were supplied by Invitrogen (Waltham, MA, USA). All chemicals were used as received without any further purification.

Preparation of CMR-MS.

CMR-MS was prepared through sol-gel co-condensation of TEOS and CMR conjugated APTS (CMR-APTS) in the presence of CTAB and NaOH. Firstly, CMR-APTS was synthesized by stirring 1 mg/mL of CMR NHS ester (N-succinimidyl 7-hydroxycoumarin-3-carboxylate) with APTS (200 µL) in CH_2Cl_2 (5 mL) in darkness for 12 h. Afterwards, ethanol (5 mL) was added to the above solution to derive 10 mL of CMR-APTS/CH_2Cl_2-ethanol solution. Next, CMR-MS was synthesized on the basis of the modified sol-gel process. Typically, CTAB (0.5 g) and Pluronic F127 (0.05 g) were first dissolved in 240 mL of deionized water, then 1.75 mL of NaOH (2 mol/L) was added followed by adjusting the solution temperature to 80 °C. After stirring for 15 min, TEOS (2.5 mL) and CMR-APTS/CH_2Cl_2-ethanol solution (5 mL) were added dropwise. The mixture was then vigorously stirred in darkness for 2 h. The resulting nanoparticles were filtered, centrifuged and washed several times with water and methanol, and CTAB was extracted by refluxing with the mixture of methanol (60 mL) and HCl (2.5 mL) for 12 h. The CMR-MS nanoparticles were centrifuged, washed thoroughly with methanol and dried under vacuum.

Preparation of AuNP and Au-6MP.

AuNP and Au-6MP were synthesized as follows. 50 mL of $HAuCl_4$ solution (0.01% by weight) was heated to boiling and 0.75 mL of trisodium citrate solution (1% by weight) was added. After being heated for 30 min, the solution was cooled to room temperature and AuNP was obtained. Au-6MP was collected by adding 6MP solution to the above AuNP solutions, and free drug was removed by centrifuging.

Preparation of Janus Bare NP and Janus 6MP NP.

Janus Bare NPs were prepared by Pickering emulsion template method with some modifications. Typically, CMR-MS (200 mg) were dispersed homogeneously in 10 mL of CTAB (1.0 µM) in 6.7% ethanol aqueous solution. The mixture was heated to 75 °C, and then paraffin (1 g) was added. When the paraffin was melted, the mixture was vigorously stirred at 23000 rpm for 10 min by a homogenizer. The resulting emulsion was further stirred for 1 h at 75 °C, then cooled to room temperature. After mixed with 10 mL of methanol, the resulting Pickering emulsion was treated with 200 µL of (3-mercaptopropyl) trimethoxysilane. The emulsion was filtered and washed with methanol after stirring for 4 h, then further dispersed in 400 mL of the corresponding Au nanoparticles aqueous solution (3 µM). The mixture was stirred overnight and then filtered and washed with deionized water. The solid was suspended in

ethanol, centrifuged, and washed three times with ethanol and three times with diethyl ether and dried under vacuum to obtain Janus Bare NP. For preparation of Janus 6MP NPs, the Au nanoparticles aqueous solution was replaced by Au-6MP solution.

Preparation of Janus Dox/6MP NP and Janus Dox NP.

Dox was conjugated to the inner surface of silica through the formation of hydrazone bonds. Briefly, adipic acid dihydrazide (52.26) mg was dissolved in DMSO (4 mL), then 3-(triethoxysilyl) propyl isocyanat (74.2 μL) in DMSO (500 μL) was added under vigorous stirring. After reacted overnight, DMSO was removed under reduced pressure at 80 °C and the waxy residue was dissolved in 2 mL of ethanol. Next, 40 mg of Janus 6MP NPs (for preparation of Janus Dox NP, Janus Bare NP was used instead) were dispersed in 16 mL of 95% ethanol aqueous solution, then 60 μL of the above silane-hydrazide solution in EtOH was added under stirring. The pH of the dispersion was tuned to 5 and stirred for 4 h at room temperature. Then the pH was tuned to neutral and stirred overnight. The resulting nanoparticles were washed several times by EtOH and water and dried under vacuum. 35 mg of above solids were dispersed in 15 mL of Dox in anhydrous methanol (0.33 mg/mL), and the pH of the mixture was tune to 5 by adding 3 μL of trifluoroacetic acid (TFA). After stirring in darkness for 40 h at room temperature, the mixture was washed thoroughly with methanol and dried under vacuum.

In vitro drug release.

For Dox release, 1 mg of Janus Dox/6MP NPs were suspended in different release media at 37 °C: phosphate buffer (PBS) with pH 7.4, PBS with pH 6.5 and PBS with pH 5.0 respectively. After particular time intervals, the nanoparticles were centrifuged and the concentration of Dox in the supernate was analyzed by QM 40 fluorescence spectrophotometer (Photo Technology International, Inc. (PTI), USA). The emission and excitation slit widths were set at 5 nm with $\lambda ex = 480$ nm. For 6MP release, 1 mg of Janus Dox/6MP NPs were suspended in PBS with 5 mM GSH at 37 °C. At predetermined time points, the nanoparticles were centrifuged and resuspended in PBS, then they were analyzed by both Laser Raman spectrometer (XploRA Laser Raman spectrometer, HORIBA JobinYvon, France) and UV-Visible spectrophotometer (Hitachi UV 2910 UV-Visible spectrophotometer). For Raman tests, aqueous solutions of different samples were loaded into capillaries and the Raman spectra were attained using a 785 nm excitation laser and a microscope with a 50x objective lens.

Cell culture.

HeLa cells were cultured in DMEM supplemented with 10% FBS and 1% streptomycin/penicillin. Cell cultures were kept at 37 °C in a 5% CO_2 humidified incubator.

Confocal imaging.

LysoTracker green DND-26 (MolecularProbes, USA) was used to stain the acidic compartments (lysosomes) in live cells. Briefly, HeLa cells were cultured on 35 mm glassbottom dishes (MatTeck, USA) in DMEM for 24 h. After that, cells were treated with Janus Dox/6MP NP (100 μg/mL) and incubated for the desired time. At the designated time point, the culture medium was removed, the cells were washed three times with PBS and visualized using a $C2^+$ Laser Scanning Confocal Microscope (Nikon, Japan).

Live cell Raman spectroscopy.

HeLa cells were cultured on 18 mm coverslips for 24 h in DMEM cell culture medium. Cells were then treated with Janus Dox/6MP NP (100 μg/mL) and incubated for 4 h, then the culture medium was removed, and the cells were washed three times with PBS. Then the cells were detected by DFM equipped Raman spectrometer, the time when injection of 5 mM of GSH-OEt was set as 0 min. The Raman spectra were attained using a 785 nm excitation laser and a microscope with a 50x objective lens.

Cell viability.

CCK-8 assays were employed to determine the cytotoxicity of various concentrations of nanoparticles on HeLa or MDA-MB-231 cells. After incubating cells with nanoparticles for 48 h, cells were washed with PBS, CCK-8 reagent was added to each well, and 3 hours later absorbance was measured using ELx800 absorbance reader (Biotek, USA) at 450 nm. The cell viability was calculated as follows: Viability= $(A_{treated}/A_{control}) \times 100\%$, where $A_{treated}$ was the absorbance of the cells treated by nanoparticles and $A_{control}$ was the absorbance of the cells without any treatments.

Characterization.

The morphology of nanoparticles was observed on a Tecnai G2 20 TWIN transmission electron microscope (FEI, USA) with an accelerating voltage of 200 kV. For sample preparation, diluted suspension was dropped on a copper grid and allowed to dry slowly. Size distribution of nanoparticles dispersed in DI water (pH 7.0) was measured by a ZS 90 Zetasizer Nano instrument (Malvern Inst. Ltd., UK) equipped with DLS (He-Ne laser, 633 nm wavelength). FTIR spectra were collected for the powders as KBr disks on a Nicolet 6700 FTIR spectrometer (Thermofisher, USA), sixty-four scans were collected per sample. Nitrogen adsorption-desorption measurements were conducted to obtain information on the porosity. The measurements were conducted at 77 K with ASAP 2420 and Micromeritcs Tristar 3020 analyzer (USA). Before measurements, the samples were degassed in vacuum at 120 °C for at least 12 h. The specific surface areas were calculated using the BET method. The pore volumes and pore size

distributions were obtained by using the BJH model from the adsorption branches of isotherms.

Acknowledgements

Notes and references

1. P. Yang, S. Gai and J. Lin, *Chem. Soc. Rev.*, 2012, **41**, 3679-3698.
2. J. Shi, Y. Jiang, X. Wang, H. Wu, D. Yang, F. Pan, Y. Su and Z. Jiang, *Chem. Soc. Rev.*, 2014, **43**, 5192-5210.
3. E. Terreno, F. Uggeri and S. Aime, *J. Control. Release*, 2012, **161**, 328-337.
4. H. Xu, Q. Li, L. Wang, Y. He, J. Shi, B. Tang and C. Fan, *Chem. Soc. Rev.*, 2014, **43**, 2650-2661.
5. J. Tang, B. Kong, H. Wu, M. Xu, Y. Wang, Y. Wang, D. Zhao and G. Zheng, *Adv. Mater.*, 2013, **25**, 6569-6574.
6. Y. Zhang, T. Shen, X. Deng, Y. Ma, L. Wang, Y. Peng, J. Wu, Z. Zhang, W. Liu and Y. Tang, *J. Mater. Chem. B*, 2015, **3**, 8449-8458.
7. M. Kim, K. Ock, K. Cho, S. W. Joo and S. Y. Lee, *Chem. Commun.*, 2012, **48**, 4205-4207.
8. B. Kang, M. M. Afifi, L. A. Austin and M. A. El-Sayed, *ACS Nano*, 2013, **7**, 7420-7427.
9. J. Lai, B. P. Shah, E. Garfunkel and K. B. Lee, *ACS Nano*, 2013, **7**, 2741-2750.
10. H. Abramczyk and B. Brozek-Pluska, *Chem. Rev.*, 2013, **113**, 5766-5781.
11. J. Huang, C. Zong, H. Shen, Y. Cao, B. Ren and Z. Zhang, *Nanoscale*, 2013, **5**, 10591-10598.
12. J. Liu, J. Bu, W. Bu, S. Zhang, L. Pan, W. Fan, F. Chen, L. Zhou, W. Peng, K. Zhao, J. Du and J. Shi, *Angew. Chem.*, 2014, **126**, 4639-4643.
13. J. Lehar, A. S. Krueger, W. Avery, A. M. Heilbut, L. M. Johansen, E. R. Price, R. J. Rickles, G. F. Short Iii, J. E. Staunton, X. Jin, M. S. Lee, G. R. Zimmermann and A. A. Borisy, *Nat Biotech*, 2009, **27**, 659-666.
14. S. Zhou, H. Sha, B. Liu and X. Du, *Chemical Science*, 2014, **5**, 4424-4433.
15. C. F. Chin, S. Q. Yap, J. Li, G. Pastorin and W. H. Ang, *Chemical Science*, 2014, **5**, 2265-2270.
16. Y. Fang, G. Zheng, J. Yang, H. Tang, Y. Zhang, B. Kong, Y. Lv, C. Xu, A. M. Asiri, J. Zi, F. Zhang and D. Zhao, *Angew. Chem.*, 2014, **126**, 5470-5474.
17. Y. Zhang, Q. Yin, J. Yen, J. Li, H. Ying, H. Wang, Y. Hua, E. J. Chaney, S. A. Boppart and J. Cheng, *Chem. Commun.*, 2015, **51**, 6948-6951.
18. J. Zhang, S. Li, F. F. An, J. Liu, S. Jin, J. C. Zhang, P. C. Wang, X. Zhang, C. S. Lee and X. J. Liang, *Nanoscale*, 2015, **7**, 13503-13510.
19. A. Jana, K. S. P. Devi, T. K. Maiti and N. D. P. Singh, *J. Am. Chem. Soc.*, 2012, **134**, 7656-7659.
20. X. Li, L. Zhou, Y. Wei, A. M. El-Toni, F. Zhang and D. Zhao, *J. Am. Chem. Soc.*, 2014, **136**, 15086-15092.
21. J. Hu, S. Zhou, Y. Sun, X. Fang and L. Wu, *Chem. Soc. Rev.*, 2012, **41**, 4356-4378.
22. A. Walther and A. H. E. Müller, *Chem. Rev.*, 2013, **113**, 5194-5261.
23. F. Wang, G. M. Pauletti, J. Wang, J. Zhang, R. C. Ewing, Y. Wang and D. Shi, *Adv. Mater.*, 2013, **25**, 3485-3489.
24. P. Díez, A. Sánchez, M. Gamella, P. Martínez-Ruíz, E. Aznar, C. de la Torre, J. R. Murguía, R. Martínez-Máñez, R. Villalonga and J. M. Pingarrón, *J. Am. Chem. Soc.*, 2014, **136**, 9116-9123.
25. C. H. Lee, S. H. Cheng, I. P. Huang, J. S. Souris, C. S. Yang, C. Y. Mou and L. W. Lo, *Angewandte Chemie International Edition*, 2010, **49**, 8214-8219.
26. S. Y. Li, L. H. Liu, H. Z. Jia, W. X. Qiu, L. Rong, H. Cheng and X. Z. Zhang, *Chem. Commun.*, 2014, **50**, 11852-11855.
27. K. Ock, W. I. Jeon, E. O. Ganbold, M. Kim, J. Park, J. H. Seo, K. Cho, S. W. Joo and S. Y. Lee, *Anal. Chem.*, 2012, **84**, 2172-2178.
28. S. Mura, J. Nicolas and P. Couvreur, *Nat. Mater.*, 2013, **12**, 991-1003.
29. Y. Wang, M. S. Shim, N. S. Levinson, H. W. Sung and Y. Xia, *Adv. Funct. Mater.*, 2014, **24**, 4206-4220.

Nanoscale Accepted Manuscript